A major purpose of the Technical Information Center is to provide the broadest dissemination possible of information contained in DOE's Research and Development Reports to business, industry, the academic community, and federal, state and local governments.

Although a small portion of this report is not reproducible, it is being made available to expedite the availability of information on the research discussed herein.

LA-UR-86-4346

CONF 861074--3

Los Alamos National Laboratory is operated by the University of California for the United States Department of Energy under contract W-7405-ENG-36

MASTER

TITLE STAGE IV WORK HARDENING IN CUBIC METALS

LA-UR--86-4346

DE87 003756

AUTHOR(S) A. D. Rollett, U. F. Kocks, and R. D. Doherty

SUBMITTED TO The Metallurgical Society, AIME, As "Formability and Metallurgical Structure", Orlando, FL, October 1986

DISCLAIMER

Los Alamos Los Alamos National Laboratory
Los Alamos, New Mexico 87545

FORM NO 836 R4
ST NO 2629 5/81

STAGE IV WORK HARDENING IN CUBIC METALS

A. D. Rollett, U. F. Kocks, and R. D. Doherty*

Center for Materials Science
Los Alamos National Laboratory
Los Alamos, New Mexico 87545

*Drexel University
Philadelphia, PA 19104

Abstract

The work hardening of f.c.c. metals at large strains is discussed with reference to the linear stress-strain behavior often observed at large strains and known as Stage IV. The experimental evidence shows that Stage IV is a work hardening phenomenon that is found quite generally, even in pure f.c.c. metals subjected to homogeneous deformation. A simple model for Stage IV in pure metals is presented, based on the accumulation of dislocation debris. Experiments are described for large strain torsion tests on four aluminum alloys. The level and extent of Stage IV scaled with the saturation stress that would represent the end of Stage III in the absence of a Stage IV. Reversing the torsion after large prestrains produced transient reductions in the work hardening. The strain rate sensitivity was also measured before and during the transient and found not to vary significantly. The microstructure observed at large strains in an Mg alloy suggest that Stage IV can occur in the absence of microband formation. Previous proposals for the cause of Stage IV are reviewed and found to be not supported by recent experimental data.

Introduction

The various stages of work hardening from easy glide on were originally defined by Diehl in 1956 (1) as Stage I for easy glide, Stage II for linear hardening and Stage III for approximately parabolic hardening. Stage IV as discussed here is usually thought of as the small but sustained hardening that occurs at very large strains, e.g. as observed in wire-drawing of iron by Langford and Cohen (2), Fig. 1.* The experimental evidence reviewed

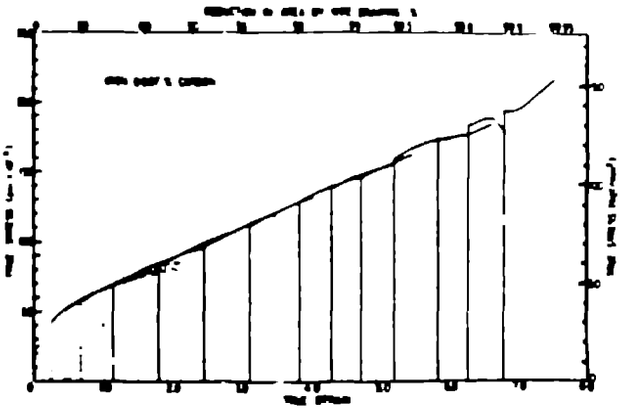

Figure 1. Stress-strain curve for wire-drawn iron obtained from successive tensile tests of wire-drawn material, from Langford and Cohen (2).

below strongly suggests that the non-zero hardening of Stage IV is a real phenomenon in various metals and alloys. It is, however, only significant at low homologous temperatures. In Ge and Si there is even a further Stage V that has been observed by Brion et al. (5). In metals, however, we will only consider Stage V to be the end of Stage IV. The various stages of work hardening are most clearly distinguished on a diagram of θ versus σ, where $\theta = \partial\sigma/\partial\varepsilon$, Fig. 2. Stage II, when present, plots as a constant, high value

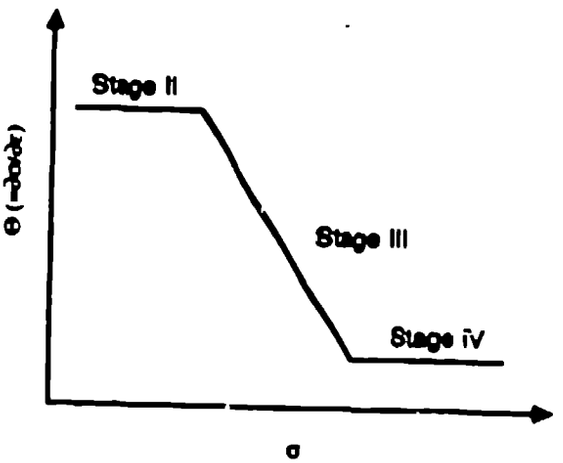

Figure 2. Diagram of hardening rate, θ, versus stress, showing the stage of work hardening for polycrystals. Stage IV plots as a straight line parallel to the stress axis.

*The reference to a "Stage IV" by Kocks (3) in 1966, referred, by contrast, to a saturation stage when Stage III is assumed to be strictly parabolic (4).

of θ at about $\mu/200$. Stage III can be represented by the Voce law which plots as a straight line where the hardening rate decreases linearly with stress towards a "saturation stress". Stage IV intervenes before the saturation stress is reached and is commonly thought of as another stage of constant, low θ at about $10^{-4}\mu$.

Recent major reviews of large-strain deformation and work hardening were published by Gil-Sevillano et al. in 1981 (6) and by Hecker and Stout in 1982 (7). Hecker and Stout emphasized the effects of impurities in increasing work hardening at large strains and suggested that torsion in pure f.c.c. metals would not show Stage IV. A corollary to the latter suggestion is the idea that Stage IV might be the result of inhomogeneous deformation such as redundant work in wire drawing or shear bands in rolling, for example. Stage IV has now been found, however, in pure Ni by Hughes (8), pure Cu by Alberdi (9) and by ourselves in 99.99% Al, all in torsion.

Mecking and Grinberg (10) discussed a number of possible causes for Stage IV. The review presented below shows that none of the causes they listed appears to be an adequate explanation of the Stage IV work hardening observed in the homogeneous torsion experiments mentioned above. In the following we first review an empirical criterion for Stage IV, due to Embury and Mecking (11). In the light of this criterion, a simple model for Stage IV is presented, based on the accumulation of dislocation debris. Then the list of possible causes of Stage IV compiled by Mecking and Grinberg (10) is reviewed. The results of current experiments on a number of aluminum alloys are presented and discussed in relation to the review.

An Empirical Criterion for Stage IV

It has been pointed out by Mecking and Embury (11) that the onset of Stage IV and the hardening rate in Stage IV, can be well fitted empirically by the criterion,

$$\theta_{IV} = c\tau_s \qquad (1)$$

where τ_s is the extrapolated stress for the end of Stage III and c is a constant of order 0.1. Figure 3 shows data from Alberdi (9) for copper tested in torsion at five different temperatures, where a choice of $c = 0.1$ gives a good fit to the transition from Stage III to Stage IV. For the higher temperatures, the hardening rate in Stage IV appears to rise with stress until it eventually decreases again towards zero. Figure 4 shows data from Hughes (8) for three Ni-Co alloys tested in torsion at two temperatures. In this case a choice of $c = 0.05$ in Eq. 1 best describes the transition to Stage IV. In contrast to Alberdi's data, the hardening rate in Stage IV of the Ni alloys is either constant or decreasing.

Dislocation Hardening

The criterion is of the same form as the Considère criterion for diffuse necking in tension. The analogy cannot be taken any further, however, since it is not obvious what instability could predict such a low factor. An alternative explanation is that the level of strain hardening observed in Stage IV is closely related to that in Stage III. Stage IV always occurs close to the saturation point of the Stage III flow stress, in other words when athermal hardening is nearly balanced by dynamic recovery (13,17). If the dislocation rearrangement that produces dynamic recovery also led to an accumulation of some different debris, a finite hardening rate would be expected to remain.

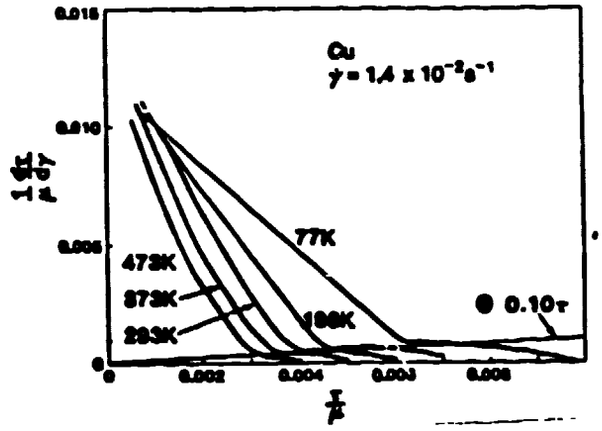

Figure 3. Hardening rate versus resolved shear stress for copper tested in torsion at five different temperatures, from Alberdi (9). Both quantities have been normalized by the temperature dependent shear modulus. Eq. 1 is plotted as straight line through the origin with slope 0.1.

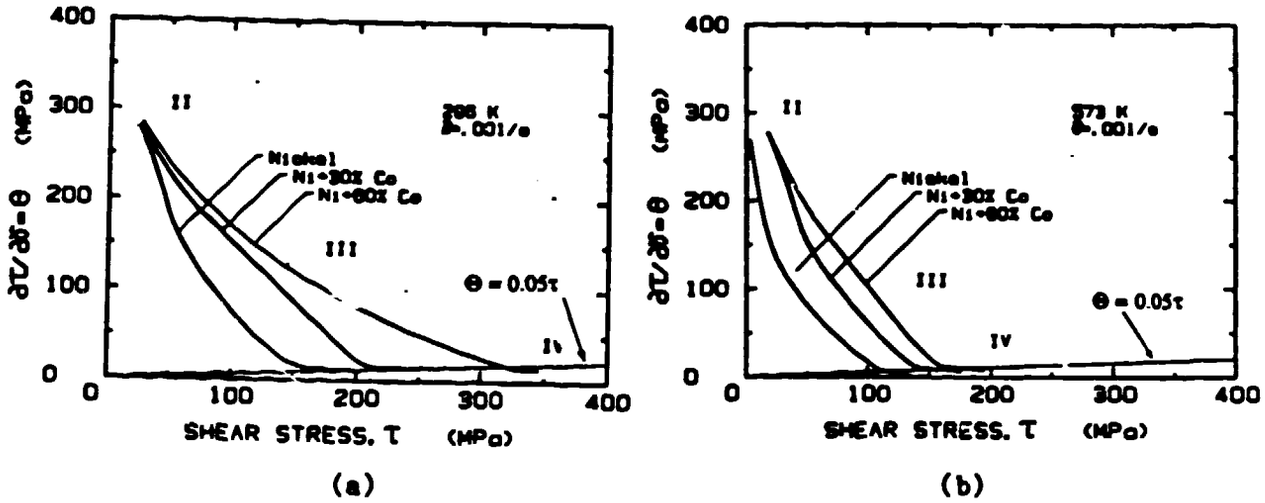

Figure 4. Hardening rate versus resolved shear stress for three Ni alloys, a) at room temperature and b) at 300 C. Equation 1 is plotted as a straight line through the origin with slope 0.05, from Hughes (8).

Many investigators have noted that monotonically strained metals develop dislocation structures that have "debris" in the form of small loops and short dipoles (12). These are in addition to the major features such as tangles or cell walls. In fact, they tend to occur inside the cell walls of metals that form cells, such as pure copper and aluminum. This debris could be the result of dynamic recovery processes and so the rate of production of debris should be at a maximum near the saturation stress. For example, a dipole might form where two dislocations of the same slip system but opposite sign would annihilate were it not for the fact that they lie on slightly separated slip planes. It seems possible that the steady accumulation of such debris might be responsible for the non-zero work hardening rate in Stage IV.

Stage III has been approximately described in phenomenological terms by

Kocks (13) as a linear decrease of hardening rate, θ, as a function of stress:

$$\theta = \theta_o (1 - \sigma/\sigma_s) \tag{2}$$

The relationship works best at moderate strains but deviations in the direction of a less rapid decrease of θ have often been observed, e.g. (14). The theoretical attempts to describe this will not be discussed here, but see, e.g., (15).

As a generalization of Eq. 2, the work hardening rate in Stage III may be written as (16),

$$\theta = \theta_o - \theta_r(\dot{\varepsilon}, T, \sigma) \tag{3}$$

The flow stress, σ, is related to the dislocation density, ρ, by the well-established relation,

$$\sigma = \alpha\mu b\sqrt{\rho} \tag{4}$$

where α is a geometrical constant of order one, μ is the shear modulus and b is the magnitude of the Burgers vector. Then the rate of change of dislocation density with strain, $\partial\rho/\partial\varepsilon$, is given by (17)

$$\frac{\partial\rho}{\partial\varepsilon} = \frac{2\sigma}{(\alpha\mu b)^2}\theta \tag{5}$$

If the rate of accumulation of debris, $\partial\rho_d/\partial\varepsilon$, is some fraction, f, of the dynamic recovery rate of dislocation density loss, then

$$\frac{\partial\rho_d}{\partial\varepsilon} = f\frac{2\sigma}{(\alpha\mu b)^2}\theta_r \tag{6}$$

Near the saturation of Stage III, the dynamic recovery rate will be approximately equal to θ_o and therefore approximately constant. Therefore the debris accumulation rate can be written as

$$\frac{\partial\rho_d}{\partial\varepsilon} = f\frac{2\sigma}{(\alpha\mu b)^2}\theta_0 = f\frac{2\sigma_s}{(\alpha\mu b)^2}\frac{\mu}{200} = \text{constant} \tag{7}$$

If the principal effect of debris accumulation is to increase the saturation stress, σ_s, then Eq. 2 can be differentiated to show that at large stresses,

$$\theta = \theta_{IV} = \partial\sigma_s/\partial\varepsilon \tag{8}$$

Comparing Eqs. 7 and 5 suggests that,

$$\theta_{IV}/\theta_o = f \tag{9}$$

The fraction, f, can be estimated at the transition from Stage III to Stage IV since at this point, the flow stress is approximately equal to the saturation stress. The ratio of the current work hardening rate to the athermal, Stage II, hardening rate then defines f. Comparison with room

temperature experiments suggests that f is of the order of 1/50, since θ_{IV} is typically of order $10^{-4}\mu$ (18). The variation of θ_{IV} with σ_s would suggest that the fraction f also scales with the saturation stress. The effect of incorporating a gradual increase of the saturation stress is illustrated in Fig. 5 by plots of hardening rate versus stress for a material with properties like those of aluminum. The upper curve illustrates the effect of a constant increase of saturation stress. The effect of an increase proportional to the level of dynamic recovery, θ_r, is illustrated by the lower curve and shows a sharper transition from Stage III to Stage IV. The curves were generated by using Eq. 2, modified to take account of a σ_s that increases with strain.

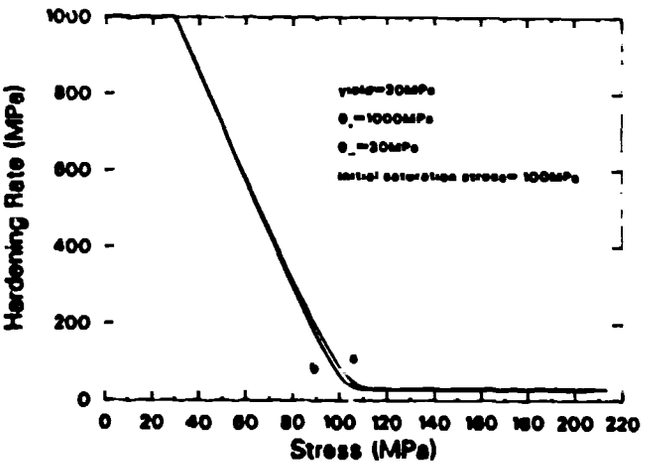

Figure 5. Work hardening rate versus stress for a material with properties similar to those of aluminum, a) constant increase of σ_s, b) increase of σ_s proportional to θ_r.

Dipoles ought to be subject to elimination by climb at sufficiently high fractions of the melting point. This model raises the interesting possibility that there is some temperature at which diffusion is strong enough to eliminate Stage IV by recovering the structure faster than debris can be accumulated. At this temperature, the level of work hardening in Stage IV should be highly rate sensitive. Models of work hardening based on diffusional recovery have been reported, e.g. (18,19), but they have been directed at Stage III work hardening. The discussion presented here only regards diffusional recovery as significant for Stage IV.

If indeed there is debris being stored that does not contribute to the flow stress, then the stored energy (proportional to the dislocation density, hence flow stress squared) should rise faster than the square of the flow stress. This has been shown to be true experimentally by the careful calorimetry of Rönnpagel and Schwink, (20).

Other Causes of Stage IV

Mecking and Grinberg (10) listed eight possible causes of Stage IV as follows:

1) Grain Size: Many alloys exhibit an increase in flow stress with decrease in grain size. Since the spacing between grain boundaries in at least one direction decreases to very small dimensions at very large strains, Stage IV might be a manifestation of grain boundary strengthening. The analogy here is with the case of hard second phases discussed above. Jago and Hansen

(21) have recently shown, however, for pure iron that the grain size effect tends to vanish, even at the relatively small tensile strain of 0.2. Hughes (8) compared the strain hardening of two different grain sizes of Ni-30Co out to large torsional strains, Fig. 6, and found also that the grain size effect tended to vanish at large strains. The reverse torsion experiments described below also tend to contradict a grain size cause for Stage IV.

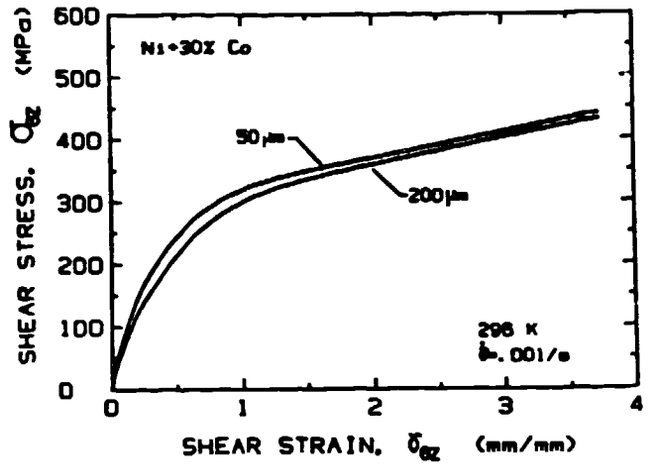

Figure 6. Stress versus strain for two different grain sizes, 50 and 200 microns of Ni-30%Co alloy, from Hughes (8).

2) Deformation Bands: Hatherly and Malin (22) defined deformation bands as the regions of a grain where slip has occurred homogeneously Deformation bands are separated by transition bands where the lattice orientation changes from that of one deformation band to the orientation of the deformation band on the other side of the transition band. Mecking and Grinberg (10) hypothesized that when the deformation bands decreased in size to dimensions comparable with the cell size, the hardening in the cell structure might be affected.

A related topic is that of misorientation between cells which tend to increase with strain. Alberdi (9) investigated both copper and aluminum and found that the misorientation increased up to 10° by a shear strain of 4 in Al. At larger strains, however, there appeared not to be any further increase in misorientation. It is possible that 10° misoriented cell walls might act as barriers to dislocation motion. Such large obstacles would, however, act as athermal obstacles and not contribute to the rate sensitivity of the material. To set against this, it is known experimentally that the rate sensitivity tends to increase during Stage IV (8,9).

3) Surface Effects: Samples deformed to large strains often have large surface-to-volume ratios. It is known, however, that the presence of a surface tends to soften a metal see Fourie (23). The anticipated effect of surfaces, therefore, would be to diminish the strain hardening at large strains.

4) Stress-Induced Transformations: In certain materials, such as the stainless steels, a phase transformation can occur at stresses elevated by strain, causing enhanced hardening. This is, however, not relevant to Stage IV in pure metals.

5) Changing Strain Path: If the relative amount of redundant strain varies, as it might in a wire drawing process for example, it is possible that the hardening might vary. It is hard, however, to see how it could lead to the sustained hardening of Stage IV and it does not explain the occurrence of Stage IV in torsion experiments.

6) Plastic Instabilities: Plastic instabilities such as shear bands often develop at large strains. Whereas macroscopic plastic instabilities tend to lead to a reduction in load bearing capacity, it seems reasonable to suppose that hardening still occurs on a microscopic scale within shear bands. It is possible, therefore, that continual shear banding could sustain hardening in a way that the prior homogeneous deformation could not (11). That is to say, the prior homogeneous deformation would saturate at a certain flow stress except that shear banding intervenes and leads to sustained hardening. For this reason, careful attention is paid to homogeneous deformation in this discussion.

7) Texture: Large plastic strains at low homologous temperatures lead to strongly developed crystallographic textures. It has been argued that as the orientation of each grain changes, so the combination of active slip systems changes. This argument depends on the latent hardening of inactive slip systems being greater than the currently active ones as is generally true. Then when a change of active slip systems occurs, the flow stress will rise. Latent hardening, however, is known to be predominant at small strains (24); this has not been investigated at the large strains discussed here. Also most grains re-orient to a stable orientation so this effect would be expected to saturate and not lead to any work hardening at very large strains.

8) Second-Phases: The presence of second phase particles of high aspect ratio provides a special case. High strains lead to decreasing spacings between the second phase particles in at least one direction. If the second phase is hard enough to block dislocation flow in the matrix then the mean free path for dislocation motion decreases strongly with strain. As the mean free path decreases, the flow stress rises by the Hall-Petch effect. If strain is measured as logarithmic strain, then the decrease in spacing is an exponential function of the strain. Embury and Fisher (25) demonstrated this type of hardening behavior in a heavily-drawn pearlitic steel and Bevk (26) more recently demonstrated this in drawn Cu-Nb alloys where the second phase was in the form of filaments. This special case of Stage IV will not be discussed further in this paper.

Torsion Tests on Al Alloys

Four different Al alloys have been tested to large strains in torsion using a short tubular specimen, Fig. 7. Torsion tests to large strains have the major advantage over other techniques that the tests are continuous tests at a uniform strain rate. They are also free of problems with lubrication and redundant work. The short tube specimen has the merit of being very stable to large strains while giving uniform plastic deformation in the gauge length (27). The testing was performed in an MTS servo-hydraulic testing machine that has been fully described elsewhere (28). This machine permits "free-end" torsion testing in the sense that any axial stresses that would develop in "fixed-end" testing are accommodated by operating the machine under axial load control. The constraint of the grip-end sections, however, does not permit the short gauge length to change diameter, so axial straining is actually prevented by volume constancy during plastic deformation. This was verified on several specimens by use of a shadowgraph before and after a test. The four alloys were 1) 99.99% pure Al, 2) Al with 0.4 atomic percent Mn, 3) Al with 2 atomic percent Mg

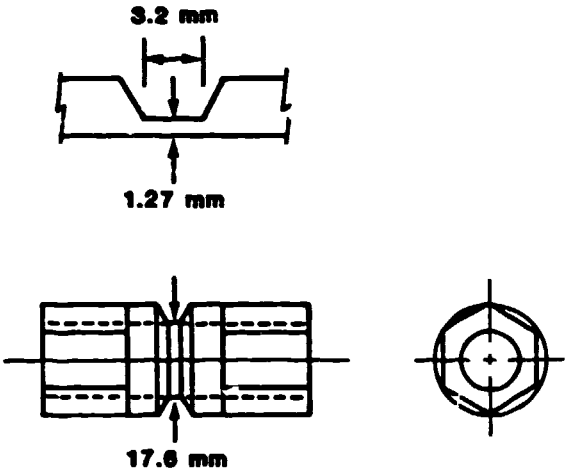

Figure 7. Design of short tube torsion specimen.

and 4) Al with 2 atomic percent Cu. The 99.99% Al is free of second phases but has enough solute that recrystallization does not occur at room temperature. The Mn alloy was heat treated to precipitate as much of the Mn as possible, in the form of coarse Al_6Mn particles. The Mg alloy contains the maximum amount of solute that is possible at room temperature. The Cu alloy was used in the over-aged state for comparison with the Mn alloy.

Stress-Strain Behavior

Figure 8 shows representative stress-strain curves for the four alloys converted to equivalent stress and equivalent strain on the basis of the von Mises yield criterion. The unalloyed Al saturates at a low stress level and the Mn alloy shows similar behavior at a somewhat higher stress level. The Mg alloy, however, reaches higher stresses and displays a clearly linear stress-strain behavior at large strains. The Cu alloy also shows sustained hardening at large strains and at an even higher stress level. Figure 9

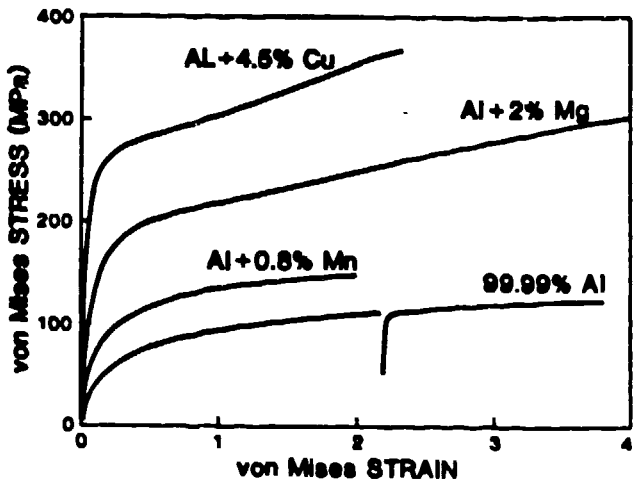

Figure 8. Stress-strain curves for four aluminum alloys, 99.99% Al, Al-0.4%Mn, Al-2%Mg and Al-2%Cu. A factor of $\sqrt{3}$ has been used to convert shear stress and strain to equivalent stress and equivalent strain.

shows a plot of hardening rate versus resolved flow stress for the four alloys. The empirical criterion of Eq. 1 for the transition to Stage IV again provides a reasonable fit to the data. The exception is the Mn alloy which shows an essentially continuous decrease in hardening down to a saturation stress. The 99.99% Al also lacks a definite Stage IV though there is a clear departure from the smooth decrease in hardening down to saturation. The Mg alloy, however, shows a clear transition to constant work hardening in Stage IV which persists to the largest strain tested, (equivalent) strain = 5. It is worth noting that the hardening tends to decrease slowly as the stress rises in Stage IV although there is sometimes an initial increase. The overaged Cu alloy also displays a transition but with slightly increasing hardening during Stage IV. Such an increasing hardening rate is in agreement with other work on alloys with semi-continuous second phase, e.g. Bevk's data for Cu with Nb filaments (26).

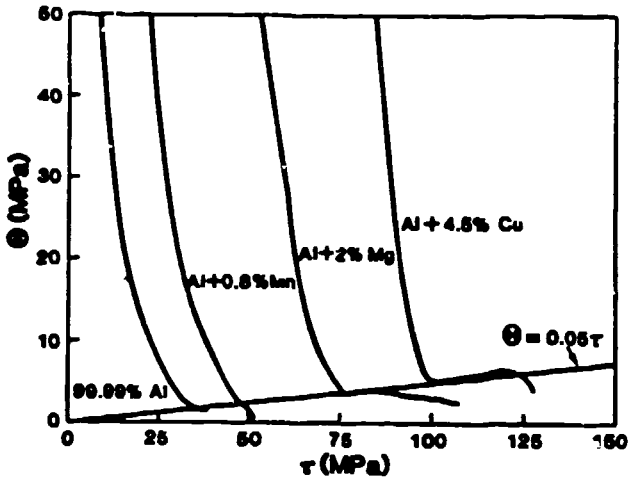

Figure 9. Hardening rate versus resolved shear stress, calculated from the data shown in Figure 8.

Torsion - Reverse Torsion

Reversing the sense of deformation has produced some interesting results in the Al alloys. Figure 10 shows stress-strain curves for the four alloys where the materials have been twisted to an equivalent strain of 2 (except for the case of the Cu alloy) and then reverse twisted to zero net strain. The reverse torsion curves have been plotted by inverting both the stress and the strain axes so as to facilitate comparison with the forward curves. In general the results show that there is little change in flow stress on reversing the deformation, except for the Cu alloy where the hard particles can support back stresses. There is also a transient during which the work hardening is zero or negative followed by hardening that is indistinguishable from the forward torsion. Such transients in work hardening have been found by other workers at smaller strains for tension-compression experiments, e.g. (29). The Mg alloy in particular shows that Stage IV is not eliminated by reversing the flow. This would appear to contradict any explanation of Stage IV based on grain boundary effects since Backofen (30) showed that the grain shape is restored on reversing the torsion. He also showed that the torsion texture is stable on reversing the flow; this means that the torsion-reverse torsion test is unusually suitable for large strain Bauschinger tests. That is, any change in flow stress or work hardening must be due to the substructure rather than to textural effects. An interesting correlation with the mechanical data was found by Iyer and

Gordon (31) who measured a transient decrease in stored energy during a compression test of Cu that had been prestrained 30% in tension.

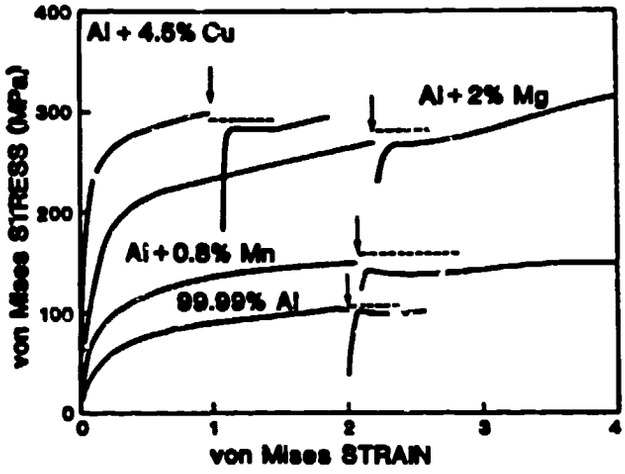

Figure 10. Effective stress-effective strain curves for the four Al alloys tested in torsion and then reverse torsion. The point at which the torsion was reversed is indicated by an arrow. The extent of the transient of reduced work hardening is indicated by a horizontal dashed line over each curve.

Strain rate jump tests were performed for the 99.99% Al and the Mg alloy for both torsion and reverse torsion. The Mg alloy displayed essentially zero rate sensitivity throughout the test, including during the work hardening transient. The 99.99% Al, however, showed a large positive rate sensitivity which increased with flow stress and again was largely unaffected by the reversal of plastic flow, Fig. 11. These results suggest that major changes in strain path might be expected to lead to changes in hardening rate with little change in rate sensitivity. Such information may be useful for studies of strain localization which sometimes involve strain path changes.

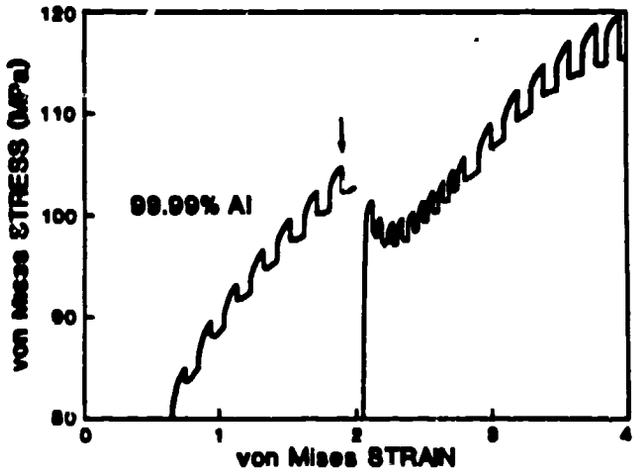

Figure 11. Equivalent stress-equivalent strain curve for 99.99% Al tested in torsion and reverse torsion with strain rate changes of a factor of 10. The point at which the torsion was reversed is indicated by an arrow.

Microstructure

Figure 12 compares the dislocation structures at an equivalent strain of 2 in the four alloys. The 99.99% Al shows a well-developed cell structure as might be expected, without pronounced directionality. The Mn alloy shows coarse precipitates of Al_6Mn which have cell walls associated with them. The cell structure appears to be somewhat finer than the precipitate spacing. The Mn remaining in solution clearly has little effect on the dislocations at room temperature, as expected from the very low mobility of Mn atoms in Al at this temperature. The Mg alloy shows a quite different microstructure with only faint cellular contrast and pronounced dislocation tangling. At this strain, the Mg alloy is well into Stage IV so it is interesting to note the apparent lack of association between the end of Stage III and the development of cells. The microstructure also lacks the intersecting microbands observed in higher Mg content Al alloys by Korbel et al. (32).

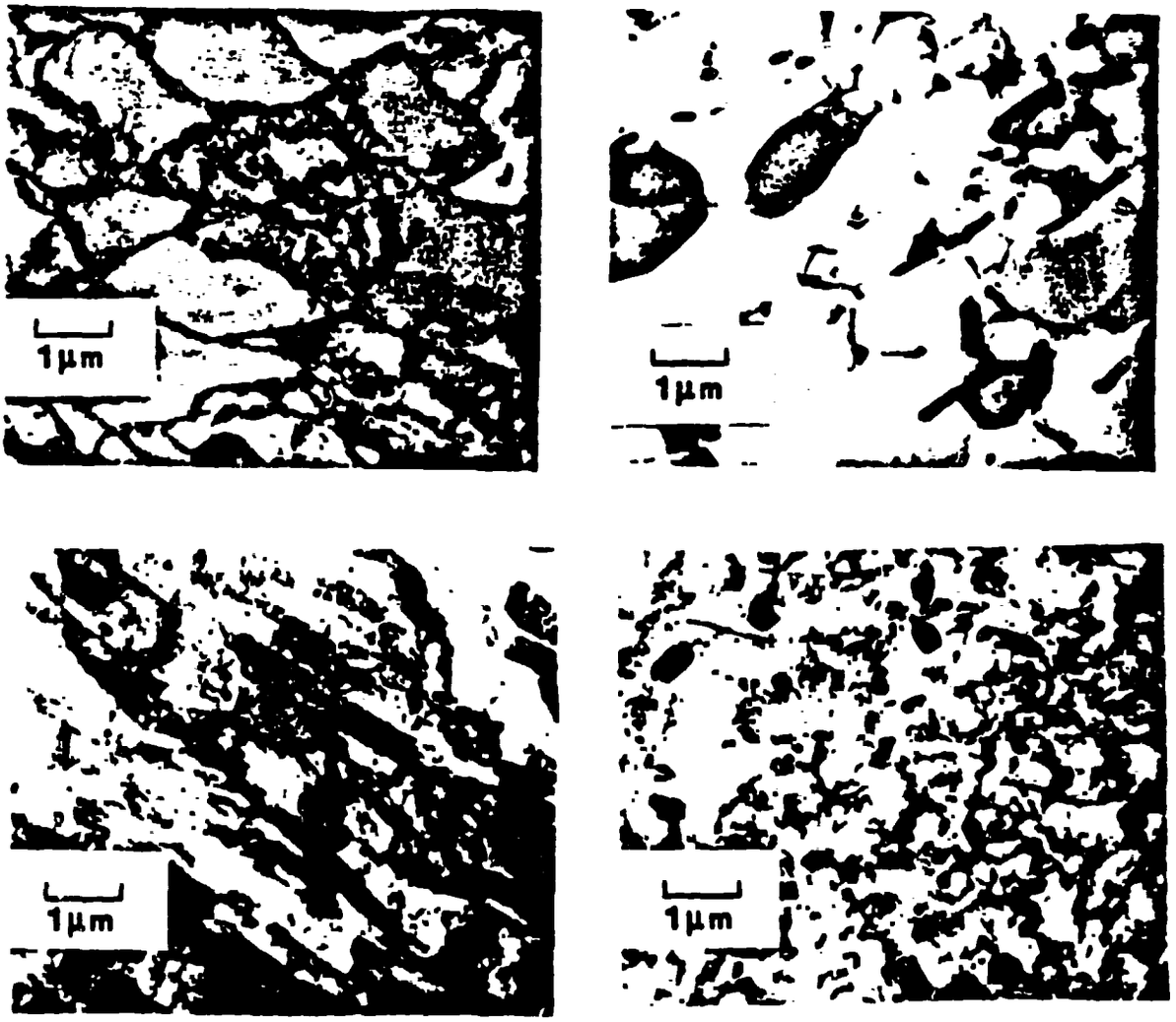

Figure 12. TEM micrographs showing the microstructures at an effective strain of 2 for 1) 99.99% Al, b) Al-0.4%Mn, c) Al-2%Mg, and d) Al-2%Cu.

The Cu alloy shows a mixture of heavily buckled plates of Al_2Cu (θ') and areas where the plates are comparatively straight. There are also instances where a colony of plates has been sheared, Fig. 13.

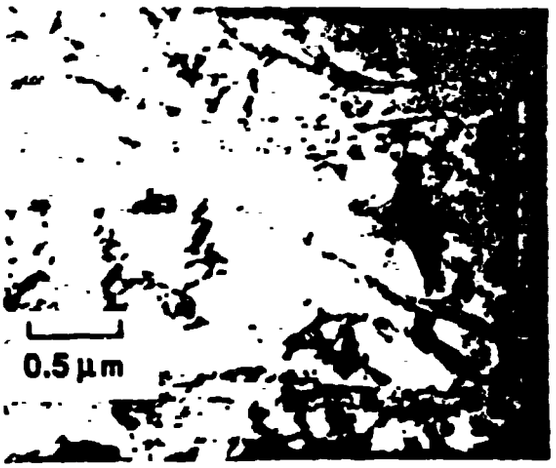

Figure 13. TEM micrograph showing θ' particles of Al_2Cu sheared by a microband.

Conclusions

Experiments on various single-phase and two-phase Al alloys confirm that Stage IV is a general phenomenon in f.c.c. metals and alloys and does occur in homogeneous torsion.

TEM observations on a Al+2% Mg alloy suggest that Stage IV can occur in a single phase alloy without the appearance of microbands in the microstructure. Hecker and Stout (7) reached the same conclusion in their discussion of hardening of heavily rolled Ni.

An analysis of all the recent data shows that there is an empirical correlation between the hardening rate at which Stage IV starts and the stress at that point. This correlation can be understood in terms of a simple debris accumulation model. This model also predicts that Stage IV should be absent at temperatures that are high enough for thermal (diffusional) recovery to eliminate the debris. This model is in agreement with the scant data available.

A number of previous proposals (10) for the cause of Stage IV were reviewed and found not to be in agreement with recent experimental data.

The effect of a reversal of strain direction on Stage IV was investigated. It was found that transients in the work hardening occur but that Stage IV reappears after the transients. The strain rate sensitivity appeared to be unaffected by the alteration in strain direction.

Acknowledgements

The authors are indebted to J. D. Embury and H. Mecking for many fruitful discussions. The assistance of M. G. Stout and M. Lovato was invaluable in obtaining the torsion data.

References

1. J. Diehl, Z. Metall., 47, p. 331 (1956).

2. G. Langford and M. Cohen, Trans. ASM, 62, p. 623 (1969).

3. U. F. Kocks, H. S. Chen, D. A. Rigney and R. J. Schaefer, Conf. on Work Hardening, AIME, Chicago, 46, p. 151 (1966).

4. D. Kuhlmann-Wilsdorf, Work Hardening, AIME, Chicago, 46, p. 97 (1966).

5. H. G. Brion, P. Haasen, and H. Siethoff, ICSMA-7, 7th Int. Conf. Strength Metals & Alloys, Pergamon, H. J. McQueen et al., eds., 1, p. 15 (1985).

6. J. Gil Sevillano, P. van Houtte and E. Aernoudt, Progress in Materials Science, 25, pp. 69-412 (1981).

7. S. S. Hecker and M. G. Stout, in Deformation, Processing and Structure, G. Krauss (ed.), ASM, St. Louis, 1982, pp. 1-46.

8. D. Hughes, Ph.D. thesis, Stanford Univ., California, (1986).

9. J. M. Alberdi G., Large Plastic Deformations in Polycrystalline Cu and Al at Low Temperatures, Ph.D. thesis, University of Navarra, Spain (1984).

10. H. Mecking and A. Grirberg, ICSMA-5, Int. Conf. on the Strength of Metals and Alloys, P. Haasen et al., eds., 1, p. 289 (1979).

11. J. D. Embury and H. Mecking, private communication, (1985).

12. P. R. Swann, in Electron Microscopy and Strength of Crystals, G. Thomas and J. Washburn (eds.), Interscience, New York, 1963, pp. 131-181.

13. U. F. Kocks, J. of Eng. Materials and Technology, 98, pp. 76-85 (1976).

14. D. J. Lloyd, B. D. McLaughlan and H. Sang, Scripta Met., 11, pp. 297-300 (1977).

15. Y. Estrin and H. Mecking, Acta Met., 32, pp. 57-70 (1984).

16. H. Mecking and U. F. Kocks, Acta Met., 29, pp. 1865-1875 (1981).

17. H. Mecking, in Work Hardening in Tension and Fatigue, A. W. Thompson, ed., AIME, New York, p. 67 (1977).

18. W. D. Nix, J. C. Gibeling and D. A. Hughes. Met. Trans, 16A, pp. 2215-2226(1985).

19. F. B. Prins and A. S. Argon, Acta Met., 32, pp. 1021-1028 (1984).

20. D. Ronnpagel and C. Schwink, Acta Met., 26, pp. 319-331 (1978).

21. R. A. Jago and N. Hansen, Acta Met., 34, pp. 1711-1720 (1986).

22. M. Hatherly and A. S. Malin, Metals Tech., 6, p. 308 (1979).

23. J. T. Fourie, ICSMA-7, 7th Int. Conf. Strength of Metals and Alloys, Pergamon, H. J. McQueen et al., eds., 1, p. 99 (1985).

24. P. Franciosi, Acta Met., 33, pp. 1601-1612 (1985).

25. J. D. Embury and R. M. Fisher, Acta Met., 14, pp. 147-159 (1966).

26. J. Bevk, Ann. Rev. Mater. Sci., 13, pp. 319-338 (1983).

27. U. S. Lindholm, A. Nagy, G. R. Johnson and J. M. Hoegfeldt, Trans ASME, J. of Eng. Mat. & Tech., 102, p. 376 (1980).

28. M. G. Stout, S. S. Hecker and R. Bourcier, Trans. ASME, J. of Eng. Mat. & Tech., 105, p. 242 (1983).

29. T. Hasegawa and T. Yakou, Scripta Met., 8, pp. 951-954 (1974).

30. W. A. Backofen, Trans AIME, 188, p. 1454 (1950).

31. A. S. Iyer and P. Gordon, Trans AIME, 215, p. 729 (1959).

32. A. Korbel, J. D. Embury, M. Hatherly, P. L. Martin and H. W. Erbsloh, Acta Met., 34, p. 1999 (1986).